Highly Efficient and Robust Au/MgCuCr$_2$O$_4$ Catalyst for Gas-Phase Oxidation of Ethanol to Acetaldehyde

Peng Liu* and Emiel J. M. Hensen*

Department of Chemical Engineering and Chemistry, Eindhoven University of Technology, 5600 MB Eindhoven, The Netherlands

S *Supporting Information*

ABSTRACT: Gold nanoparticles (AuNPs) supported on MgCuCr$_2$O$_4$-spinel are highly active and selective for the aerobic oxidation of ethanol to acetaldehyde (conversion 100%; yield ~95%). The catalyst is stable for at least 500 h. The unprecedented catalytic performance is due to strong synergy between metallic AuNPs and surface Cu$^+$ species. X-ray photoelectron spectroscopy shows that Cu$^+$ is already formed during catalyst preparation and becomes more dominant at the surface during ethanol oxidation. These Cu$^+$ species are stabilized at the surface of the ternary MgCuCr$_2$O$_4$-spinel support. Further kinetic measurements indicate that the Cu$^+$ species act as sites for O$_2$ activation.

Production of chemicals and fuels from abundant, renewable biomass and its derivatives provides a viable route to alleviate our strong dependence on depleting fossil fuels.[1] For this purpose, ethanol (EtOH) is particularly attractive because of its facile synthesis by biomass fermentation and expected increased availability and reduced cost.[2] Selective oxidation of ethanol to acetaldehyde (AC), acetic acid, and ethyl acetate is of great interest for the chemical industry to decrease the use of petrochemical reserves.[3] In particular, AC is an important bulk chemical for the production of peracetic acid, pentaerythritol, pyridine bases, butylene glycol, and chloral, with a worldwide production over 10^6 tons/year.[4] Currently, production of AC is mainly by the Wacker process, via oxidation of ethylene in strong acidic solutions catalyzed by palladium and copper chlorides.[5] Here, a promising opportunity arises to replace petroleum-based ethylene by renewable ethanol for more green and sustainable AC production.

Recently, the use of supported gold nanoparticles (AuNPs) to catalyze aerobic oxidation of alcohols has become the center of attention.[6] AuNP catalysts have, in particular, shown promise for selective oxidation of ethanol with molecular oxygen.[7−15] Liquid-phase ethanol oxidation mainly yields acetic acid or ethyl acetate, but supported AuNP catalysts suffer deactivation upon reuse due to gold sintering under hydrothermal conditions.[7] A more attractive process for industrial application would be gas-phase ethanol oxidation because of the convenience of catalyst separation, solvent-free conditions, and facile continuous process operation.[16] The most significant disadvantage of current gold-based catalysts would appear to be the high reaction temperature, which tends to cause low selectivity and deactivation. For instance, Stucky reported that 6.3 nm Au/SiO$_2$ showed an EtOH conversion of 45% with 75% AC selectivity at 200 °C.[10] Au/TiO$_2$

(~2 nm) was able to convert 60% of an ethanol feed at ~120 °C; full conversion was reached at 280 °C, but under these conditions the catalyst gradually deactivated and selectivity was below 80%.[12] Among various unitary oxide-supported AuNP catalysts, Au/MoO$_3$ showed the highest AC yield (>90% at 240 °C), but without evidence of catalyst stability.[14] More recently, pre-oxidized bimetallic Au−Cu/SiO$_2$ catalysts were reported to be active and stable for EtOH conversion (~90%) with ~85% AC selectivity at 200 °C for 50 h on-stream.[15] However, these catalysts are far from practical application, mainly because of the low EtOH concentration (<1 vol%),[14] the low AC selectivity (<90%),[10−13,15] and/or the low gas hourly space velocity (GHSV < 10,000 mL g$_{cat}^{-1}$ h^{-1}).[10,12,13,15]

In this Communication, we present a ternary spinel (MgCuCr$_2$O$_4$)-supported AuNP catalyst that is capable of achieving ~100% EtOH conversion with ~95% AC selectivity at 250 °C of a feed of 1.5 vol% EtOH at a GHSV of ~100,000 mL g$_{cat}^{-1}$ h^{-1}. The catalyst is very stable for at least 500 h (Figure 1). The unprecedented catalytic performance relates to synergy between AuNP and surface Cu$^+$ species, which facilitates O$_2$
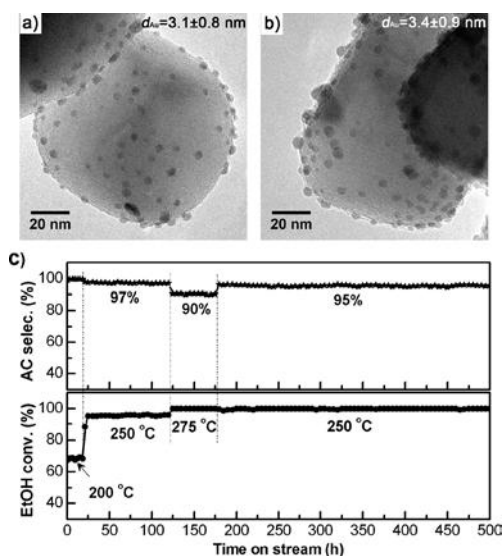

Figure 1. TEM images of (a) fresh Au/MgCuCr$_2$O$_4$ catalyst and (b) used Au/MgCuCr$_2$O$_4$ catalyst after 500 h on-stream. (c) Ethanol conversion and acetaldehyde selectivity vs time on stream using Au/MgCuCr$_2$O$_4$ (reaction conditions: catalyst 0.1 g, GHSV = 100,000 mL g$_{cat}^{-1}$ h^{-1}, EtOH/O$_2$/He = 1/3/63).

Table 1. Textural and Physicochemical Properties and Catalytic Activity Results for Various Supported Au Catalysts

entry	catalyst	S_{BET} (m²/g)	d_{Au} (nm)	$[Au]^a$ (wt%)	X^b (%)	S^b (%)	TOF $(h^{-1})^c$
1	Au/MgCr₂O₄	16	3.3	0.93	6	96	207
2	Au/MgCoCr₂O₄	26	3.2	0.97	9	98	293
3	Au/MgNiCr₂O₄	17	3.3	0.96	7	96	233
4	Au/MgCuCr₂O₄	5	3.1	0.90	68	99	2351
5	Au/CuCr₂O₄	4	3.6	0.93	40	99	1556
6	Au/MgCuAl₂O₄	158	2.5	0.83	30	98	898
7^d	Au/CuO-SiO₂	165	2.8	0.93	20	97	592
8	Au/MgAl₂O₄	152	3.4	0.78	4	99	178
9^e	Au/SiO₂	287	6.3	1.87	12	92	378
10	Au/TiO₂	50	2.2	0.98	13	91	264
11^f	Au/MgCuCr₂O₄	5	4.5	0.90	38	99	1909
12^g	Au/MgCuCr₂O₄	5	3.1	0.90	73	99	2539

^{a}Determined by ICP-OES. ^{b}EtOH conversion (X) and AC selectivity (S) at 200 °C (catalyst 0.1 g, EtOH/O₂/He = 1/3/63, GHSV = 100,000 mL g_{cat}^{-1} h^{-1}). ^{c}Turnover frequency based on acetaldehyde yield and gold dispersion ($D = 1.3/d$),[11] and given in mol$_{aldehyde}$ mol$_{surface\,Au}^{-1}$ h^{-1}. ^{d}By using CuO/SiO₂ (26.2 wt% Cu) as support. ^{e}By using Au(en)₂Cl₃ as precursor. ^{f}Catalyst was calcined at 500 °C in air for 5 h. ^{g}Pretreated in H₂ at 300 °C for 2 h.

activation. The MgCuCr₂O₄-spinel stabilizes Cu⁺ formed during catalyst preparation and ethanol oxidation and also ensures high and stable AuNP dispersion.

Chromite-spinels were chosen primarily because of the potential shown in our previous work on hydrotalcite-supported AuNP catalysts for liquid-phase aerobic oxidation of alcohols.[17] The strong synergy between MgCr-hydrotalcite and AuNP motivated us to explore the gas-phase ethanol oxidation on MgCr-based oxide (typically MgCr₂O₄-spinel)-supported gold catalysts. To date, no chromite-spinel-supported AuNP catalysts were reported for ethanol oxidation.[18] We prepared several Mg₀.₇₅M₀.₂₅Cr₂O₄-spinels (denoted as MgMCr₂O₄, M = Co, Ni, Cu) with the same structure as MgCr₂O₄ by a coprecipitation-calcination method, which was also used for the preparation of other reference spinel supports (see Supporting Information for details). All gold catalysts were prepared by the deposition–precipitation method with urea.[19] The surface area, mean AuNP size, and Au loading of the catalysts are collected in Table 1. Under identical preparation conditions, all chromite-spinels showed much lower surface area than aluminate-spinels. The very low surface area of copper-containing chromite-spinels is consistent with the presence of large crystals (see Figures S1 and S2 for XRD patterns and SEM images). Evidently, the difference in spinel surface area has little influence on gold dispersion (Figure S3), with mean AuNP sizes always being between 2 and 4 nm.

Initially, we investigated the effect of the chromite-spinels on the catalytic activity of Au/MgMCr₂O₄ in gas-phase aerobic oxidation of ethanol (Table 1, entries 1−4). At 200 °C, AC is the predominant product (selectivity >95%) in all cases. Au/MgCuCr₂O₄ outperforms non-Cu-containing catalysts (Table 1, entries 1−3) by nearly an order of magnitude, pointing to strong synergy between AuNP and the Cu-containing spinel. To identify the beneficial effect of Cu-containing oxide supports, Au/CuCr₂O₄, Au/MgCuAl₂O₄, and Au/CuO-SiO₂ catalysts were also evaluated (Table 1, entries 5−7). These catalysts showed much lower activity than Au/MgCuCr₂O₄ catalyst, despite their higher Cu content, higher surface area and smaller AuNP size. Moreover, Au/MgCuCr₂O₄ outperforms previously
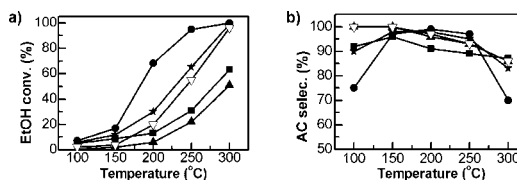

Figure 2. Temperature-dependent ethanol oxidation over various catalysts showing (a) ethanol conversion and (b) acetaldehyde selectivity. (●) Au/MgCuCr₂O₄, (★) Au/MgCuAl₂O₄, (■) Au/TiO₂, (▲) Au/MgCr₂O₄, and (▽) Au/CuO-SiO₂.

reported preferred Au/MgAl₂O₄,[7a] Au/SiO₂[10,11] and Au/TiO₂[12] catalysts for ethanol oxidation (Table 1, entries 8−10). These results clearly point to a specific gold-support interaction in Au/MgCuCr₂O₄.

Figure 2 shows the temperature dependence of EtOH conversion and AC selectivity over representative catalysts. Au/MgCuCr₂O₄ exhibited higher activity than other catalysts below 300 °C, with a dramatic activity increase after 150 °C. The selectivity to AC of Au/MgCuCr₂O₄ (see Table S1), interestingly, showed a maximum between 150 and 250 °C, with ethyl acetate as byproduct at lower temperature and acetic acid and CO₂ as main byproducts at higher temperature. Although Au/TiO₂ typically achieves moderate conversion at low temperature (~120 °C),[12] its performance is inferior to Au/MgCuCr₂O₄ at the same low temperature, mainly due to the much higher GHSV applied here (see Figure S4 for catalytic performance at lower GHSV). MgCr-spinel oxide-supported AuNP (Au/MgCr₂O₄) without Cu showed low activity even at 300 °C, indicating the importance of Au−Cu interactions.[16a] Au/MgCuAl₂O₄ and Au/CuO-SiO₂ with much higher surface area and smaller AuNP size still showed inferior activity. These results further point to the pivotal role of the chromite-spinel support.

To investigate the stability of Au/MgCuCr₂O₄, the catalyst was run for 500 h in ethanol oxidation and the results are shown in Figure 1c. The catalyst was found to be stable at 200 °C for the first 20 h, and also at 250 °C for the following 100 h, with conversion increasing to 95% and AC selectivity slightly decreasing to 97%. When the temperature was further increased to 275 °C, full conversion was achieved during 50 h, with selectivity decreasing to 90%. Interestingly, after decreasing the temperature to 250 °C, the conversion and selectivity remained at 100% and 95%, respectively, for more than 300 h. In contrast, the ethanol conversion of Au/MgCuAl₂O₄ catalyst at 200 °C decreased from 30 to 25% after 5 h. To our delight, after 500 h on-stream, the structure and morphology of the Au/MgCuCr₂O₄ catalyst was largely retained (see Figure S2 for SEM image), with the average AuNP size only slightly increased from 3.1 to 3.4 nm (Figure 1a,b). Several other reference catalysts showed significant increases in the AuNP size after 50 h on-stream (see Figure S5), pointing to the stabilizing effect of MgCuCr₂O₄ on AuNP size. These results unequivocally demonstrate the robust nature of Au/MgCuCr₂O₄ catalyst for gas-phase ethanol oxidation to acetaldehyde. Considering that prior to reaction the catalyst was pre-treated in O₂ at 300 °C and the decreased activity for catalyst with larger AuNP size (Table 1, entry 11; also see Figure S6), we surmised that the activity increase may be due to ethanol-induced changes to the active sites.

To obtain further insight into the gold−support interactions, we studied the oxidation state of Au, Cr and Cu of the fresh Au/MgCuCr₂O₄ catalyst and after catalyzing ethanol oxidation for 500 h by X-ray photoelectron spectroscopy (XPS, Figure 3). The
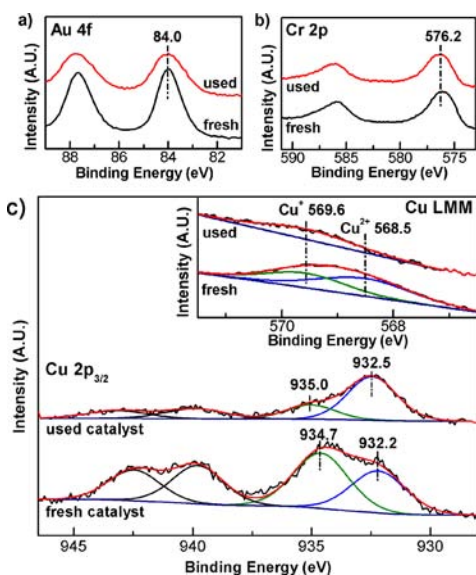
Figure 3. XP spectra of the Au/MgCuCr$_2$O$_4$ catalyst before and after 500 h on stream. (a) Au 4f XP spectra, (b) Cr 2p XP spectra, and (c) Cu 2p$_{3/2}$ and Cu LMM (inset) XP spectra.

Figure 4. (a) Ethanol conversion and (b) acetaldehyde selectivity for temperature-dependent aerobic oxidation of ethanol over (●) Au/MgCuCr$_2$O$_4$ and (■) MgCuCr$_2$O$_4$, and non-oxidative ethanol dehydrogenation over (○) Au/MgCuCr$_2$O$_4$ and (□) MgCuCr$_2$O$_4$. (c) Non-oxidative ethanol dehydrogenation performance vs time on stream using Au/MgCuCr$_2$O$_4$ (reaction conditions: catalyst 0.1 g, GHSV = 100,000 mL g$_{cat}^{-1}$ h^{-1}, ethanol/He = 1/66).

binding energy (BE) was corrected for surface charging by taking the C 1s peak of contaminant carbon as a reference at 284.5 eV. The Au 4f$_{7/2}$ BE remains constant at 84.0 eV, the value for metallic gold. Similarly, the BE of Cr 2p$_{3/2}$ was ∼576.2 eV, which is typically attributed to Cr^{3+}.[20] The Cu 2p$_{3/2}$ XP spectra (Figure 3c) are different before and after use of Au/MgCuCr$_2$O$_4$ as a catalyst. Two contributions are discerned at 935 and 932 eV. The higher BE peak at ∼935 eV is assigned to Cu^{2+} in the spinel, accompanied by the characteristic Cu^{2+} shakeup satellite peaks (938−945 eV).[21] The lower BE peak at ∼932 eV suggests the presence of Cu$^+$ or Cu^0 species.[20,21] Because Cu 2p$_{3/2}$ XPS cannot differentiate between Cu$^+$ and Cu^0, Auger Cu LMM spectra were used to confirm the presence of Cu$^+$ at BE ∼570 eV.[22] This is consistent with the fact that both the spinel support and the gold catalyst were prepared by adopting a calcination step in air, so that the presence of metallic Cu in the fresh catalyst is not likely. Interestingly, significant changes were observed when comparing Cu XP spectra of the fresh and spent catalysts, with the Cu LMM transition showing only Cu$^+$ species. The surface Cu$^+$ fraction, derived from Cu 2p$_{3/2}$ XP spectra, increased from 26 to 55% during 500 h time on stream, indicating that part of surface Cu^{2+} species are reduced to Cu$^+$ species during ethanol oxidation. To further prove the selective reduction of Cu^{2+} to Cu$^+$ in the MgCuCr$_2$O$_4$-spinel, the Au/MgCuCr$_2$O$_4$ catalyst and the MgCuCr$_2$O$_4$ support were pretreated in ethanol vapor or H$_2$ at 300 °C. XPS confirms the significantly increased surface Cu$^+$ content following these treatments and the absence of bulk Cu^0 species (see Figure S7). The surface Cu$^+$ fraction is 63% for H$_2$-reduced Au/MgCuCr$_2$O$_4$. The pre-reduced catalyst showed higher activity than the pre-oxidized one under identical conditions (Table 1, entry 12; also see Figure S8). These results further support that the synergy is related to the co-existence of Au^0 and Cu$^+$ species, and the increased catalytic performance at 250 °C after running for 50 h at 275 °C (Figure 1c) is due to enhanced Au^0−Cu$^+$ synergy. It is noteworthy that the surface Au/Cu atomic ratio in the pre-oxidized and pre-reduced Au/MgCuCr$_2$O$_4$ catalysts is similar (∼0.7) and much higher than in the other Cu-containing catalysts (see Table S2). The somewhat decreased Au/Cu ratio (∼0.6) in the spent catalyst after 500 h
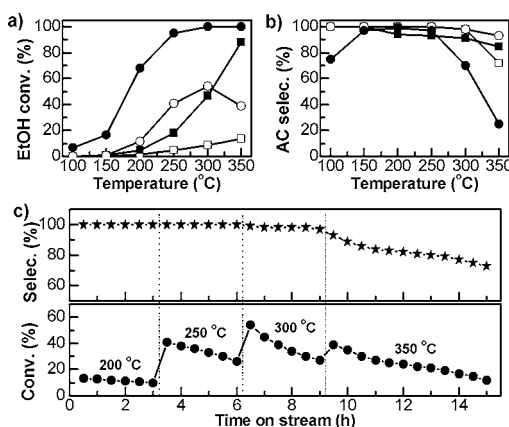
can be due to the small increase of AuNP size from 3.1 to 3.4 nm. These findings point to Au^0−Cu$^+$ interactions decreasing AuNPs sintering.

To understand the reducibility of the spinel-supported gold catalysts, we performed temperature-programmed reduction study (TPR, Figure S9). The amount of reducible species of the spinel supports and the gold catalysts derived thereof was found to be consistent with the Cu content (see Table S3). For the Au/MgCuCr$_2$O$_4$ and Au/CuCr$_2$O$_4$ catalysts, only 5.2 and 6.3% of the Cu species were reduced below 300 °C, respectively. In the case of Au/MgCuAl$_2$O$_4$, however, over 80% of Cu species was reduced below 300 °C, indicating the lower stability of Cu^{2+}/Cu$^+$ in the MgCuAl$_2$O$_4$-spinel. Although the surface Cu$^+$ fraction of fresh Au/MgCuAl$_2$O$_4$ catalyst is as high as 54%, the facile reduction of these Cu species to Cu^0 in the presence of ethanol (see Figure S10 for XPS results) results in inferior activity, presumably because of the absence of desirable Au^0−Cu$^+$ interactions. In contrast, the Au/MgCuCr$_2$O$_4$ catalyst contains no Cu^0, demonstrating the advantage of MgCr$_2$O$_4$-type spinels in stabilizing Cu^{2+}/Cu$^+$ species. On the basis of these observations, the unique promotional effect of MgCuCr$_2$O$_4$-spinel support can be attributed to (i) the possibility of reducing Cu^{2+} to Cu$^+$ without Cu^0 formation, leading to development of Au^0−Cu$^+$ synergy beneficial for ethanol oxidation and (ii) strong metal−support interactions, thus rendering robust Au/MgCuCr$_2$O$_4$ catalyst with stable AuNP size.

In an attempt to further understand the nature of Au^0−Cu$^+$ synergy and reaction mechanism, we determined the contribution of non-oxidative ethanol dehydrogenation to the total activity of aerobic ethanol oxidation. Indeed, CuO·CuCr$_2$O$_4$ (copper chromite) is known to be an active catalyst for ethanol dehydrogenation.[23] Figure 4a,b shows the activity and selectivity comparison of MgCuCr$_2$O$_4$-spinel and Au/MgCuCr$_2$O$_4$ for EtOH conversion in the presence and absence of oxygen in the feed. Over the bare MgCuCr$_2$O$_4$-spinel, negligible oxidation took place at temperatures below 200 °C, but at higher temperature AC was gradually produced accompanied by formation of ethyl acetate and CO$_2$ (see Table S4). The MgCuCr$_2$O$_4$-spinel, however, exhibited very poor activity for non-oxidative dehydrogenation of ethanol even at 350 °C, which we attribute

to the absence of Cu^0 sites for the initial O−H bond cleavage in our catalyst.[24] Figure 4c shows that $Au/MgCuCr_2O_4$ deactivates during ethanol dehydrogenation and the more so at higher temperatures, with ethylene/ethyl acetate as main byproducts. Compared with the excellent activity of $Au/MgCuCr_2O_4$ in aerobic oxidation, its low activity in dehydrogenation demonstrates the importance of O_2 for the Au^0−Cu^+ synergy. The absence of activated oxygen species as H acceptor to remove the surface adsorbed Au−H hydride and to release free Au^0 sites may be the reason for activity decreasing with the temperature and time increasing. XPS (see Figure S7) excludes the reduction of Cu^+ during non-oxidative ethanol dehydrogenation and temperature-programmed oxidation (TPO, Figure S11) confirms that rapid coking is the cause of the deactivation. In contrast, in the presence of O_2, coking is suppressed and stable performance can be achieved.

On the basis of the above observations, we propose that O_2 activation occurs on Cu^+ sites instead of AuNP. This is supported by the finding that $Au/MgCr_2O_4$ is significantly less active for ethanol oxidation than $Au/MgCuCr_2O_4$. The resulting active oxygen species (O^- or O_2^-) are thought to act as basic sites to facilitate O−H bond cleavage and metal-alcoholate formation[6] (Scheme S1). AuNP in close proximity to such centers will act as the sites for C−H cleavage, which is believed to be the most difficult step in alcohol oxidation.[11,13a,15] We speculate that the oxidized Cu^{2+}−OH intermediates can be reduced by the proximate Au−H hydride formed by C−H cleavage of adsorbed Au-alcoholate, accompanied by water formation and removal, thereby recovering the initial Cu^+ and free Au^0 active centers. This novel synergistic effect between Cu^+ and Au provides a more efficient route for ethanol oxidation to acetaldehyde than using previously reported Cu^0-containing AuCu alloy catalysts.[15,16a]

In summary, we report for the first time an approach to achieve highly efficient, selective and stable oxidation of ethanol to acetaldehyde by using $MgCuCr_2O_4$-spinel-supported gold nanoparticles. This significant progress is based on the identification of a novel and potentially broader applicable Au−Cu synergy in alcohol oxidation, likely being based on the interaction of AuNPs with Cu^+ which activate O_2. The Cu^+ species are stabilized in a chromite-spinel phase and become more dominant at the surface during the ethanol oxidation. Through interactions with the Cu^+-containing chromite-spinel the AuNPs are stable during reaction. We have already demonstrated stable ethanol oxidation operation at 250 °C (1.5 vol% ethanol and a GHSV of 100,000 mL g_{cat}^{-1} h^{-1}) for 500 h. Under these conditions, the ethanol conversion is complete and the acetaldehyde selectivity is 95%. It is therefore reasonable to state that the novel catalyst has potential for acetaldehyde production from bioethanol.

ASSOCIATED CONTENT

Ⓢ Supporting Information

Experimental details, preparation and characterization of the catalysts. These materials are available free of charge via the Internet at http://pubs.acs.org.

AUTHOR INFORMATION

Corresponding Authors

pliu503@hotmail.com
e.j.m.hensen@tue.nl

Notes

The authors declare no competing financial interest.

REFERENCES

(1) (a) Corma, A.; Iborra, S.; Velty, A. *Chem. Rev.* **2007**, *107*, 2411. (b) Alonso, D. M.; Bond, J. Q.; Dumesic, J. A. *Green Chem.* **2010**, *12*, 1493. (c) Gallezot, P. *Chem. Soc. Rev.* **2012**, *41*, 1538.

(2) (a) Rass-Hansen, J.; Falsig, H.; Jørgensen, B.; Christensen, C. H. *J. Chem. Technol. Biotechnol.* **2007**, *82*, 329. (b) Sun, J.; Zhu, K.; Gao, F.; Wang, C.; Liu, J.; Peden, C. H. F.; Wang, Y. *J. Am. Chem. Soc.* **2011**, *133*, 11096.

(3) Takei, T.; Iguchi, N.; Haruta, M. *Catal. Surv. Asia* **2011**, *15*, 80.

(4) Caro, C.; Thirunavukkarasu, K.; Anilkumar, M.; Shiju, N. R.; Rothenberg, G. *Adv. Synth. Catal.* **2012**, *354*, 1327.

(5) (a) Jira, R. *Angew. Chem., Int. Ed.* **2009**, *48*, 9034. (b) Keith, J. A.; Henry, P. M. *Angew. Chem., Int. Ed.* **2009**, *48*, 9038.

(6) (a) Hashmi, A. S. K.; Hutchings, G. J. *Angew. Chem., Int. Ed.* **2006**, *45*, 7896. (b) Pina, C. D.; Falletta, E.; Prati, L.; Rossi, M. *Chem. Soc. Rev.* **2008**, *37*, 2077. (c) Corma, A.; Garcia, H. *Chem. Soc. Rev.* **2008**, *37*, 2096. (d) Zhang, Y.; Cui, X.; Shi, F.; Deng, Y. *Chem. Rev.* **2012**, *112*, 2467.

(7) (a) Christensen, C. H.; Jørgensen, B.; Rass-Hansen, J.; Egeblad, K.; Madsen, R.; Klitgaard, S.; Hansen, S.; Hansen, M.; Andersen, H.; Riisager, A. *Angew. Chem., Int. Ed.* **2006**, *45*, 4648. (b) Jørgensen, B.; Christiansen, S. E.; Thomsen, M. L.; Christensen, C. H. *J. Catal.* **2007**, *251*, 332. (c) Tembe, S. M.; Patrick, G.; Scurrell, M. S. *Gold Bull.* **2009**, *42*, 321.

(8) Sun, K. Q.; Luo, S. W.; Xu, N.; Xu, B. Q. *Catal. Lett.* **2008**, *124*, 238.

(9) Biella, S.; Rossi, M. *Chem. Commun.* **2003**, 378.

(10) Zheng, N.; Stucky, G. D. *J. Am. Chem. Soc.* **2006**, *128*, 14278.

(11) Guan, Y.; Hensen, E. J. M. *Appl. Catal., A* **2009**, *361*, 49.

(12) (a) Simakova, O. A.; Sobolev, V. I.; Koltunov, K. Y.; Campo, B.; Leino, A.-R.; Kordás, K.; Murzin, D. Y. *ChemCatChem* **2010**, *2*, 1535. (b) Sobolev, V. I.; Koltunov, K. Y.; Simakova, O. A.; Leino, A.-R.; Murzin, D. Y. *Appl. Catal., A* **2012**, *433−434*, 88.

(13) (a) Gong, J.; Mullins, C. B. *J. Am. Chem. Soc.* **2008**, *130*, 16458. (b) Kong, X. M.; Shen, L. L. *Catal. Commun.* **2012**, *24*, 34.

(14) Takei, T.; Iguchi, N.; Haruta, M. *New J. Chem.* **2011**, *35*, 2227.

(15) Bauer, J. C.; Veith, G. M.; Allard, L. F.; Oyola, Y.; Overbury, S. H.; Dai, S. *ACS Catal.* **2012**, *2*, 2537.

(16) (a) Pina, C. D.; Falletta, E.; Rossi, M. *J. Catal.* **2008**, *260*, 384. (b) Fan, J.; Dai, Y.; Li, Y.; Zheng, N.; Guo, J.; Yan, X.; Stucky, G. D. *J. Am. Chem. Soc.* **2009**, *131*, 15568.

(17) (a) Liu, P.; Guan, Y.; van Santen, R. A.; Li, C.; Hensen, E. J. M. *Chem. Commun.* **2011**, *47*, 11540. (b) Liu, P.; Li, C.; Hensen, E. J. M. *Chem.—Eur. J.* **2012**, *18*, 12122.

(18) Sobczak, I.; Szrama, K.; Wojcieszak, R.; Gaigneaux, E. M.; Ziolek, M. *Catal. Today* **2012**, *187*, 48.

(19) Zanella, R.; Giorgio, S.; Henry, C. R.; Louis, C. *J. Phys. Chem. B* **2002**, *106*, 7634.

(20) Deutsch, K. L.; Shanks, B. H. *J. Catal.* **2012**, *285*, 235.

(21) Severino, F.; Brito, J. L.; Laine, J.; Fierro, J. L. G.; Agudo, A. L. *J. Catal.* **1998**, *177*, 82.

(22) Platzman, I.; Brener, R.; Haick, H.; Tannenbaum, R. *J. Phys. Chem. C* **2008**, *112*, 1101.

(23) Prasad, R. *Mater. Lett.* **2005**, *59*, 3945.

(24) Zhang, M.; Li, G.; Jiang, H.; Zhang, J. *Catal. Lett.* **2011**, *141*, 1104.